Hierarchical Approach for Simulation of Binary Adsorption in Silicalite

Kenneth F. Czaplewski and Randall Q. Snurr
Dept. of Chemical Engineering, Northwestern University, Evanston, IL 60208

A hierarchical molecular modeling approach presented predicts adsorption thermodynamics of single components and binary mixtures in zeolites. Atomistic simulations that capture details at the molecular level are performed to calculate the free energies of molecules at discrete adsorption sites. Then a more coarse-grained lattice model is used to calculate the equilibrium loading of adsorbates based on these free energies, and thermodynamic properties can be predicted. Sorbate–sorbate free energies beyond nearest-neighbor interactions are introduced and their impact on the lattice model is investigated. By adding these free energies, the model is better able to accurately describe single-component and binary adsorption of sulfur hexafluoride and neopentane in silicalite. The results from the lattice model agree well with full atomistic grand canonical Monte Carlo simulations performed for the same systems, but the hierarchical approach saves an order of magnitude of computational effort.

Introduction

The microporous crystalline structure of zeolites provides unique properties that make their use prevalent in many processes in the chemical and petrochemical industries. The ability to make use of these materials is dependent upon our understanding of how the sorption thermodynamics are determined by the underlying molecular-level structure and energetics. This understanding allows the improvement of current applications involving zeolites and gives insight into how they could be used in new areas. Major applications currently include catalysis, adsorption separations, waste treatment, and detergent formulation (Davis, 1991; Breck, 1974).

Virtually all industrial applications of zeolites involve multicomponent adsorption. The presence of more than one component further complicates an already challenging problem of accurately describing interactions of molecules in a heterogeneous adsorption environment. Adsorbent heterogeneity can lead to phenomena such as preferential siting of dissimilar sorbates in different sorption locations for adsorbed mixtures (Clark et al., 1998). This segregation can give rise to deviations from ideal adsorbed solution behavior (Dunne and Myers, 1994; Dunne et al., 1997). While experimentation supplies a wealth of information about multicomponent systems, a variety of theoretical approaches have also been used to model adsorption thermodynamics of mixtures in zeolites (Ruthven, 1984) and to link the macroscopic thermodynamics to the molecular structure.

Lattice models have been used for many years to describe localized adsorption in zeolites (Hill, 1956; Ruthven, 1984). The method is best suited to zeolites having discrete adsorption sites or cages connected by narrow windows. The cages are usually treated as independent subsystems, or if each site holds only one molecule, potential energy interactions between nearest-neighbor sites may be taken into account (Lee et al., 1992; Van Tassel et al., 1994a; Chiang et al., 1997; Rudzinski et al., 1997). For localized adsorption within cages or for zeolites without cages, the adsorption sites are often taken to be at minimum energy locations within the zeolite. This approach was used by Van Tassel et al. (1994a) in their study of the adsorption of xenon and methane in zeolite NaA. Lee et al. (1992) used a two-dimensional model to describe aromatic adsorption in silicalite, a zeolite without cages. Sites in the straight channels, zigzag channels, and channel intersections were considered. When sorbate interactions were considered only for nearest-neighbor sites, the grand partition function describing the system could be transformed to a two-dimensional Ising model, and an exact solution for the occupancy density was determined. To extend the model to include sorbate interactions between next nearest-neighbor

Correspondence concerning this article should be addressed to R. Q. Snurr.

sites, mean field theory was applied to obtain the fractional occupancy of each site. As with other lattice models, the model of Lee et al. contains adjustable parameters that were fit to experimental data to obtain reasonable agreement.

Adsorption in zeolites has also been modeled using atomistic representations, which are solved by large-scale computer simulations based on statistical mechanics. Atomistic grand canonical Monte Carlo (GCMC) simulations of adsorption in zeolites provide a means of calculating information at the molecular level such as siting and molecular configuration, while predicting macroscopic properties such as adsorption isotherms and heats of adsorption that often agree well with experimental results. Given a force field that describes a system well, the simulations allow one to make accurate predictions about real systems of interest. In addition to work on single-component systems, the adsorption of binary mixtures in zeolites has been investigated using atomistic GCMC simulations in several studies (Karavias and Myers, 1991; Razmus and Hall, 1991; Maddox and Rowlinson, 1993; Dunne and Myers, 1996; Van Tassel et al., 1994b, 1996; Dunne et al., 1996; Jameson et al., 1996, 1997; Lachet et al., 1997; Heuchel et al., 1997; Clark et al., 1998; Macedonia and Maginn, 1999). The adsorption of mixtures of smaller molecules such as oxygen and nitrogen in zeolite 5A and three binary systems (C_2H_4-CO_2, CH_4-CO_2, and i-C_4H_{10}-C_2H_4) in zeolite X have been simulated by Razmus and Hall (1991) and Karavias and Myers (1991), respectively. Macedonia and Maginn (1999) have examined mixtures of methane, ethane, and propane in silicalite, and *p*-xylene/*m*-xylene mixtures in faujasite zeolites have been simulated by Lachet et al. (1997).

While lattice models can be used to correlate many thermodynamic properties, they lack predictive capability due to adjustable parameters that are fit to experimental data. Atomistic models, on the other hand, provide a means to accurately describe an adsorption system, but often they cannot be applied to complex systems due to computational constraints. Taking a hierarchical approach that combines the predictive capability of an atomistic simulation and the computational efficiency of a lattice model presents itself as an attractive simulation strategy. Short atomistic simulations are used to obtain the parameters for the lattice model. The parameters describe the free energy in various adsorption sites due to interactions between an adsorbed molecule and the zeolite, as well as interactions between neighboring adsorbed molecules. These energies are then inputs to a lattice model from which the adsorption equilibrium properties of the system are determined. Snurr et al. (1994) showed that this hierarchical methodology could be applied to accurately calculate the adsorption of benzene in silicalite.

This article describes two important enhancements to the approach of Snurr et al. (1994). First, we extend it to multicomponent systems. Second, we introduce interactions between sorbates that are located in *next* nearest-neighbor sites. Such interactions were suspected to play an important role at high loadings in the work of Snurr et al. (1994). In the following sections, fully atomistic GCMC simulations of sulfur hexafluoride, neopentane, and their binary mixtures in silicalite are described first. These results serve as a basis of comparison for the hierarchical lattice model, which is then described in detail. A new expression for the free energies is derived encompassing multiple components, starting from the grand canonical partition function. A discussion of the short atomistic simulations used to calculate the free energies follows, along with a discussion of the improvements made to the lattice model incorporating these free energies. The results from the hierarchical lattice model are then compared to the full atomistic GCMC results and discussed.

Atomistic GCMC Calculations

Atomistic GCMC simulations of sulfur hexafluoride (SF_6) and neopentane adsorption in silicalite were performed using the energy-biased algorithm of Clark et al. (1998) for mixtures. The grand canonical ensemble is sampled by performing three types of moves; molecular translations, attempts to insert a molecule into the system, and attempts to remove an existing molecule from the system. A typical simulation involved between 1 and 10 million iterations per isotherm point. The simulation system consisted of 8 to 12 unit cells of silicalite. Silicalite has a three-dimensional network of pores, consisting of sinusoidal channels that intersect straight channels. Both channels are approximately 5.5 Å in diameter. The atoms that make up the zeolite impose a potential energy field upon molecules that enter the pore network during adsorption. In our model, the crystallographic positions of the silicalite atoms are assumed to be fixed in space and are taken from X-ray diffraction studies (Olson et al., 1981). The interaction of the zeolite structure with an adsorbed molecule is modeled by a pairwise-additive Lennard-Jones potential between the adsorbed molecule and the oxygen atoms of the zeolite framework. It is assumed that the effects of zeolite silicon atoms on an adsorbed molecule are shielded by those of the oxygen atoms and are therefore excluded from the potential field calculation (Kiselev et al., 1985). The Lennard-Jones parameters for the interaction of the zeolite oxygen atoms with the adsorbed molecules and among the sorbates themselves are listed in Table 1. The Lorentz-Berthelot mixing rules are used to calculate the interaction parameters for combinations of dissimilar species.

The atomistic GCMC simulations of both sulfur hexafluoride (SF_6) and neopentane in silicalite show that the single-component adsorption of these molecules occurs at discrete locations within the structure of the zeolite. This is shown in Figure 1, where the transparent outer shell represents the silicalite pore structure, displayed as a contour of constant potential energy of $+100$ kJ/mol between SF_6 and the framework oxygen. The dark shaded regions represent the most probable adsorption locations. The positions of more than 90% of the centers of mass sampled during the simulation

Table 1. Lennard-Jones Potential Parameters Used in the Simulations*

Interaction Pair	ϵ/k (K)	σ (Å)	Reference
SF_6–SF_6	222.1	5.128	Reid et al., 1987
SF_6–oxygen	147.2	3.967	June et al., 1991
SF_6—neopentane	207.3	5.796	Reid et al., 1987
Neopentane–neopentane	193.4	6.464	Reid et al., 1987
Neopentane–oxygen	131.6	4.635	Reid et al., 1987; Snurr et al., 1993

*The sorbate–sorbate values of sigma reflect the sizes of the molecules.

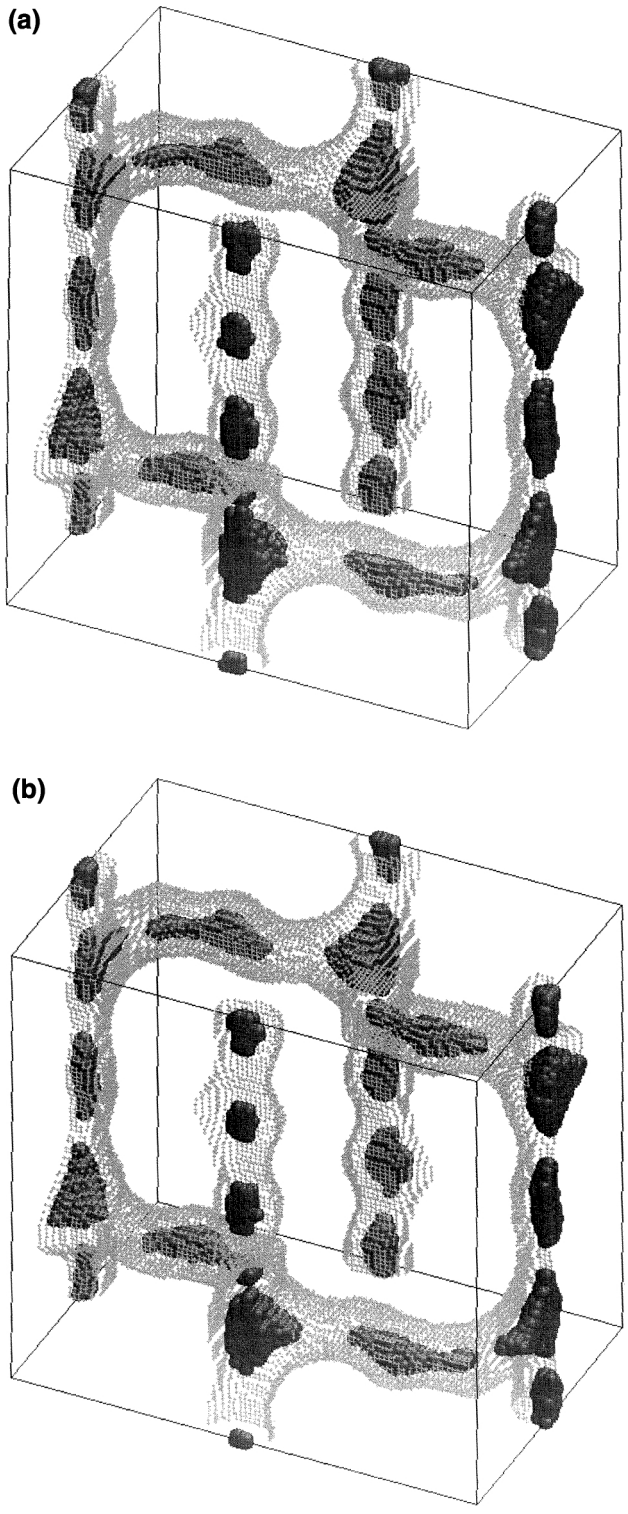

Figure 1. Probability density contour plots of SF_6 in silicalite at 293 K (a) at a loading of 8.49 molecules per unit cell, and (b) at a loading of 2.12 molecules per unit cell, generated using atomistic GCMC.

The dark regions represent the locations of 90% of the centers of mass of the molecules sampled during the simulations. The lighter outer shell represents a contour of constant potential energy of +100 kJ/mol between SF_6 and the framework oxygen.

are enclosed in these dark shaded volumes. Figure 1a displays the results of SF_6 in silicalite at high loading (8.49 molecules per unit cell, 20°C, 1.0 kPa), and Figure 1b at low loading (2.12 molecules per unit cell, 20°C, 0.1 kPa). The adsorption occurs within the channels and their intersections at discrete locations as opposed to a continuous distribution, as is observed in the adsorption of smaller molecules, such as CF_4 (Clark et al., 1998). Figure 2 shows the results of a simulation of neopentane in silicalite at high loading (3.50 molecules per unit cell, 20°C, 0.1 kPa). In this case, molecules are seen to adsorb only in the channel intersections. Atomistic GCMC simulations were also performed on binary mixtures of SF_6 with neopentane. These binary results, along with the single-component atomistic GCMC isotherms, are used below as a measure of how well the hierarchical lattice model predicts adsorption data.

Hierarchical Lattice Model

Since the atomistic GCMC simulation results show that the adsorbed molecules concentrate in localized volumes within the pore system of the zeolite, the use of a lattice model to describe the SF_6 and neopentane systems is appropriate. The atomistic GCMC simulations show the existence of three types of lattice sites corresponding to the straight channels (S), sinusoidal or zigzag channels (Z), and the channel inter-

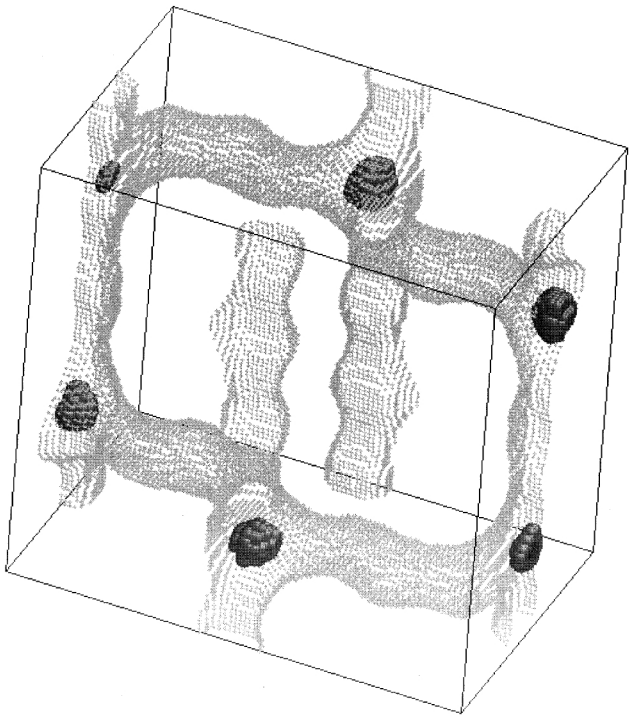

Figure 2. Probability density contour plot of neopentane in silicalite at 293 K at a loading of 3.50 molecules per unit cell generated using atomistic GCMC.

The dark volumes enclose 90% of the most likely positions occupied by the centers of mass of the neopentane molecules sampled during the simulation. The lighter outer shell represents a contour of constant potential energy of +100 kJ/mol between SF_6 and the framework oxygen.

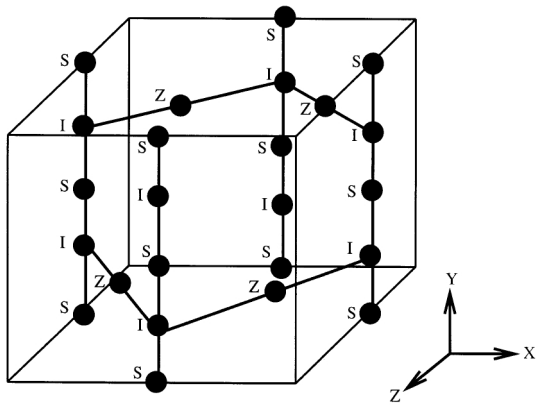

Figure 3. Lattice of adsorption sites in a unit cell of silicalite.

The spheres represent adsorption sites at the straight channels (S), the zigzag channels (Z), and the channel intersections (I). The thick lines denote the connectivity of the straight and sinusoidal channel system.

sections (I). The lattice representation of the zeolite used in our hierarchical lattice model is shown in Figure 3. The lattice is a more coarse-grained picture of the system, consisting of discrete sites that are either unoccupied or occupied with a single molecule of a given type. In this section, the lattice model is derived for multicomponent adsorption in silicalite, starting from the atomistic description. The approximations invoked in the derivation will be explicitly noted and discussed below. The grand partition function of the atomistic model is discretized in a fashion that is consistent with the localized adsorption observed in atomistic simulations in silicalite. This involves the introduction of free energies that describe the interaction between a molecule adsorbed in a lattice site and its surroundings. These free energies, which are functions of temperature, are then used in the lattice model to determine the occupancy of the lattice sites for a given gas-phase pressure and composition, and thus an adsorption isotherm can be generated.

Because our focus here is to test the importance of next nearest-neighbor interactions and to extend the hierarchical approach to mixtures for the first time, we have chosen to model two spherical sorbates to reduce the computational burden. SF_6 and neopentane were chosen as two fairly large molecules that can be reasonably approximated as spherical. Each is modeled here as a single Lennard-Jones sphere. The approach described below can be readily extended to nonspherical molecules, similar to the original hierarchical approach of Snurr et al. (1994), which was developed for an atomistic representation of benzene.

The grand partition function for a zeolite and a mixture of adsorbed molecules containing Ω components can be written as (Snurr et al., 1994; Hill, 1962)

$$\Xi(\mu_1, \mu_2, \ldots, \mu_\Omega, V, T) = \sum_{N_1=0}^{\infty} \sum_{N_2=0}^{\infty} \cdots \sum_{N_\Omega=0}^{\infty} \frac{1}{\eta} \int \exp(-\mathfrak{V}/kT)\, d\Re(q_t' \lambda'), \quad (1)$$

where the subscripts 1, 2, …, Ω indicate the components in the mixture, k is Boltzmann's constant, and V, T, and μ_i are the fixed solid-phase volume, temperature, and chemical potential of the ith component, respectively. The contribution to the partition function of the zeolite degrees of freedom is neglected, and the zeolite is only considered to provide an external potential field felt by the adsorbed molecules. The potential energy of the system, $\mathfrak{V}$, is a function of the positions of all the molecules, $\boldsymbol{r}$, and incorporates the potential energy between the zeolite and the sorbate and between the adsorbed molecules; N_i is the total number of indistinguishable molecules of the ith component in the system; and

$$\frac{1}{\eta} = \prod_{\omega=1}^{\Omega} \frac{1}{N_\omega!}; \qquad d\Re(q_t', \lambda') = \prod_{\omega=1}^{\Omega} d^{3N_\omega} r\left(q_{t_\omega} \lambda_\omega\right)^{N_\omega}. \quad (2)$$

The η term accounts for the identical and indistinguishable nature of molecules of the same type. The integration of the translational degrees of freedom, $\Re$, is performed for each molecule in the mixture over the entire solid-phase volume. The absolute activity, λ_i, is defined as $\exp(\mu_i/kT)$, and the kinetic energy factor, along with other energetic terms such as nuclear or electronic, are incorporated in the q_t' factor.

Since the molecules of the system can be considered as being adsorbed in lattice sites, the summations in Eq. 1 over the number of indistinguishable molecules can be replaced with summations over the distinguishable sites, each of which can contain at most one molecule of the Ω components of the system

$$\Xi = \sum_{i_1=0}^{\Omega} \sum_{i_2=0}^{\Omega} \cdots \sum_{i_{n_I}=0}^{\Omega} \sum_{j_1=0}^{\Omega} \sum_{j_2=0}^{\Omega} \cdots \sum_{j_{n_S}=0}^{\Omega} \sum_{k_1=0}^{\Omega} \sum_{k_2=0}^{\Omega} \cdots \sum_{k_{n_Z}=0}^{\Omega} \times \int \exp(-\mathfrak{V}/kT)\, d\Re(q_t' \lambda'), \quad (3)$$

where n_I, n_S, and n_Z are the total numbers of I, S, and Z sites constituting the total volume, V. The index i_ℓ ($\ell = 1, \ldots, n_I$) represents the type of molecule adsorbed ($i_\ell = 1, 2, \ldots, \Omega$) in the ℓth site of type I. If the site is unoccupied, i_ℓ is equal to zero to represent the vacancy of the site. The indices j_ℓ ($\ell = 1, \ldots, n_S$) and k_ℓ ($\ell = 1, \ldots, n_Z$) have similar meanings for the adsorption in sites of type S and type Z, respectively. For example, $j_3 = 2$ denotes the occupancy of the third straight channel adsorption site with a single molecule of the second component of the mixture, while $k_2 = 0$ denotes a vacancy in the second zigzag channel. The total number of molecules in the system, N, is given by Eq. 4.

$$N = \sum_{\omega=1}^{\Omega} \sum_{\ell=1}^{n_I} \delta(i_\ell - \omega) + \sum_{\omega=1}^{\Omega} \sum_{\ell=1}^{n_S} \delta(j_\ell - \omega) + \sum_{\omega=1}^{\Omega} \sum_{\ell=1}^{n_Z} \delta(k_\ell - \omega), \quad (4)$$

where $\delta(x_l - \omega)$ is the Dirac delta function. Now, rather than summing over the total number of indistinguishable molecules, the partition function has been transformed into a

summation over the distinguishable sites, $\{i_1, \ldots, i_{n_I}, j_1, \ldots, j_{n_S}, k_1, \ldots, k_{n_Z}\}$, which compose the total volume of the system. The integration of the translational degrees of freedom of each molecule is now carried out over the volume of the site occupied by the molecule in the considered configuration. The possibility of more than one component being present has also been accounted for. To represent this transformation, the following abbreviated notation can be used:

$$\Xi = \sum_{\{i,j,k\}}^{\Omega} \int \exp(-\mathfrak{V}/kT)\, d\Re(q_t'\lambda'). \tag{5}$$

The following assumptions are now invoked in order to simplify the derivation of the lattice model. Upon completion, these assumptions will be revisited. The first assumption is that sorbates only interact with each other if they occupy nearest-neighbor sites. The next assumption is that the system is dilute enough so that any given molecule has at most one single neighbor. The integration is now performed over single isolated occupied sites and over pairs of nearest-neighbor occupied sites. The first three terms of the partition function in Eq. 6 are for I, S, and Z sites that contain a single isolated molecule of component ω. The last two terms are for pairs of molecules of type ω and χ in nearest-neighbor I and Z sites and I and S sites, respectively. These assumptions and the connectivity of the sites in silicalite limit the number of possible combinations of interactions between adsorbed molecules to the following:

$$\begin{aligned}\Xi = \sum_{\{i,j,k\}}^{\Omega} &\left[\int_{\{I_\omega\}} \exp(-\mathfrak{V}_\omega^{zs}/kT)\, d^3r_\omega\right]^{N'_{I_\omega}} \\ &\times \left[\int_{\{S_\omega\}} \exp(-\mathfrak{V}_\omega^{zs}/kT)\, d^3r_\omega\right]^{N'_{S_\omega}} \\ &\times \left[\int_{\{Z_\omega\}} \exp(-\mathfrak{V}_\omega^{zs}/kT)\, d^3r_\omega\right]^{N'_{Z_\omega}} \\ &\times \left[\int_{\{I_\omega Z_\chi\}} \exp(-\mathfrak{V}_{\omega\chi}/kT)\, d^3r_\omega\, d^3r_\chi\right]^{N_{I_\omega Z_\chi}} \\ &\times \left[\int_{\{I_\omega S_\chi\}} \exp(-\mathfrak{V}_{\omega\chi}/kT)\, d^3r_\omega\, d^3r_\chi\right]^{N_{I_\omega S_\chi}} (q_{t_\omega}\lambda_\omega)^{N_\omega},\end{aligned} \tag{6}$$

where N'_{I_ω}, N'_{S_ω}, N'_{Z_ω} represent the number of isolated molecules of type ω adsorbed in the I, S, and Z sites, respectively; $N_{I_\omega S_\chi}$ and $N_{I_\omega Z_\chi}$ are the number of pairs of molecules of types ω and χ occupying nearest-neighbor I and S sites or I and Z sites; and N_ω is the total number of adsorbed molecules of the ωth component defined in Eq. 7:

$$\begin{aligned} N_\omega &= N_{I_\omega} + N_{S_\omega} + N_{Z_\omega} \qquad N_{I_\omega} = N'_{I_\omega} + \sum_{\chi=1}^{\Omega} \left(N_{I_\omega S_\chi} + N_{I_\omega Z_\chi}\right) \\ N_{S_\omega} &= N'_{S_\omega} + \sum_{\chi=1}^{\Omega} N_{I_\chi S_\omega} \qquad N_{Z_\omega} = N'_{Z_\omega} + \sum_{\chi=1}^{\Omega} N_{I_\chi Z_\omega} \end{aligned} \tag{7}$$

The partition function now contains two different potential energies, $\mathfrak{V}_\omega^{zs}$, for the isolated molecules that only include the zeolite/sorbate interaction, and $\mathfrak{V}_{\omega\chi}$, for pairs of molecules that consist of the zeolite/sorbate interaction energy for both species and the sorbate/sorbate potential energy between the two molecules; $\mathfrak{V}_{\omega\chi} = \mathfrak{V}_\omega^{zs} + \mathfrak{V}_\chi^{zs} + \mathfrak{V}_{\omega\chi}^{ss}$.

Based on these expressions, a configurational free energy, A_{I_ω}, is defined for an isolated molecule of type ω in an intersection site:

$$\exp\left[-\frac{A_{I\omega}}{kT}\right] = \frac{1}{V_{uc}} \int_{\{I_\omega\}} \exp(-\mathfrak{V}_\omega^{zs}/kT)\, d^3r_\omega, \tag{8}$$

where V_{uc} is the volume of the unit cell of silicalite and serves as a normalization factor. Isolated molecules of type ω in straight channel sites and in zigzag channel sites also have free energies defined similarly, A_{S_ω}, and A_{Z_ω}. The values of these free energies can be determined by directly evaluating the configurational integral defined in Eq. 8 for a single molecule adsorbed in a specific site using the same atomistic model used in the atomistic GCMC simulations described in the previous section. The values of A_{I_ω}, A_{S_ω}, and A_{Z_ω} are also taken as the zeolite/sorbate contribution to the free energy for pairs of molecules in adjacent sites, and a free energy, $A_{I_\omega S_\chi}$ is defined for the sorbate/sorbate interaction between a molecule in an intersection and a molecule in a straight channel

$$\exp\left[\frac{-A_{I_\omega S_\chi} - A_{I_\omega} - A_{S_\chi}}{kT}\right] = \frac{1}{(V_{uc})^2} \int_{I_\omega S_\chi} \exp(-\mathfrak{V}_{\omega\chi}/kT)\, d^3r_\omega\, d^3r_\chi, \tag{9}$$

where A_{I_ω} and A_{S_χ} are defined in Eq. 8. The free energy $A_{I_\omega Z_\chi}$ is defined in a similar fashion for a pair of molecules occupying an intersection and a zigzag channel. By evaluating the configurational integral defined in Eq. 9 for a pair of molecules adsorbed in two adjacent sites, the values of these sorbate/sorbate free energies are determined. Finally, the definitions of the free energies are substituted back into the partition function defined in Eq. 6, and since $q_{t_\omega}\lambda_\omega = f_\omega/kT$, where f_ω is the fugacity of the ωth component, we can write:

$$\Xi = \sum_{\{i,j,k\}}^{\Omega} \left(\frac{f_\omega V_{uc}}{kT}\right)^{N_\omega} \exp\left(-\frac{\left(N_{I_\omega}A_{I_\omega} + N_{S_\omega}A_{S_\omega} + N_{Z_\omega}A_{Z_\omega} + N_{I_\omega S_\chi}A_{I_\omega S_\chi} + N_{I_\omega Z_\chi}A_{I_\omega Z_\chi}\right)}{kT}\right). \tag{10}$$

This is the desired expression for the grand canonical partition function of a lattice model for describing the adsorption of a mixture in silicalite. The adsorption sites are either occupied with a single molecule of the mixture or vacant, and this

information for all sites completely specifies the state of the system. The zeolite/sorbate and sorbate/sorbate free energies are used to calculate the energy of any given state of the system. These free energies are calculated ahead of time from the atomistic model by the direct evaluation of the configurational integral over the volume of the adsorption site, Eqs. 8 and 9, thus integrating away all of the molecular detail. The free energies thus provide a link between the atomistic detail required to accurately predict adsorption properties and the more coarse-grained lattice picture, which is much more computationally efficient.

We now address the assumptions made previously in the derivation. The first assumption was to ignore sorbate/sorbate interactions beyond those of nearest neighbors. Interactions extending beyond nearest neighbors can be systematically added to the model as necessary. We extended the derivation to include sorbate/sorbate interactions between *next* nearest neighbors and determined the free-energy contribution. For example, if two intersections were occupied with adsorbed molecules of any type, regardless of the occupancy of the site in the center, an S or Z site, the sorbate/sorbate contribution to the free energy, $A_{\mathrm{I\_I}}$, was tabulated:

$$\exp\left[\frac{-A_{\mathrm{I}_\omega-\mathrm{I}_\chi}-A_{\mathrm{I}_\omega}-A_{\mathrm{I}_\chi}}{kT}\right] = \frac{1}{(V_{uc})^2}\int_{\mathrm{I}_\omega\mathrm{I}_\chi}\exp\left(-\mathbb{V}_{\omega\chi}/kT\right)d^3r_\omega\, d^3r_\chi, \quad (11)$$

where A_{I_ω} and A_{I_χ} are the zeolite/sorbate free energies of isolated molecules of types ω and χ, respectively, occupying intersection sites. All of the possible combinations of next nearest neighbors, S__S, Z__Z, and S__Z, were examined and their sorbate/sorbate free energies determined.

The second assumption was that the system was at very low loading, and therefore only single occupied sites or lone pairs of occupied sites existed. This assumption was modified by further extending the model to include the interactions of triplets of molecules and calculating the three-body free energies of three molecules adsorbed in adjacent sites. For example, if adjacent intersection, straight, and intersection sites were occupied, the contribution of this triplet to the free energy of the system, $A_{\mathrm{I}_\omega\mathrm{S}_\chi\mathrm{I}_\delta}$, was determined.

$$\exp\left[\frac{-A_{\mathrm{I}_\omega\mathrm{S}_\chi\mathrm{I}_\delta}-A_{\mathrm{I}_\omega}-A_{\mathrm{S}_\chi}-A_{\mathrm{I}_\delta}-A_{\mathrm{I}_\omega\mathrm{S}_\chi}-A_{\mathrm{I}_\delta\mathrm{S}_\chi}-A_{\mathrm{I}_\omega-\mathrm{I}_\delta}}{kT}\right] = \frac{1}{(V_{uc})^3}\int_{\mathrm{I}_\omega\mathrm{S}_\chi\mathrm{I}_\delta}\exp\left(-\mathbb{V}_{\omega\chi\delta}/kT\right)d^3r_\omega\, d^3r_\chi\, d^3r_\delta, \quad (12)$$

where $\mathbb{V}_{\omega\chi\delta}$ is the total potential energy of the triplet of molecules consisting of the zeolite/sorbate interaction energies of the three molecules and the three sorbate/sorbate potential energies between the three molecules; $\mathbb{V}_{\omega\chi\delta} = \mathbb{V}_\omega^{\mathrm{zs}} + \mathbb{V}_\chi^{\mathrm{zs}} + \mathbb{V}_\delta^{\mathrm{zs}} + \mathbb{V}_{\omega\chi}^{\mathrm{ss}} + \mathbb{V}_{\delta\chi}^{\mathrm{ss}} + \mathbb{V}_{\omega\delta}^{\mathrm{ss}}$. Similar 3-body free energies have been defined for the other triplets of molecules, SIS, IZI, ZIZ, and SIZ. To use the model at even higher loadings where more than three adjacent occupied sites exist, it is assumed that the multiple sorbate free energies are still valid and that the interactions between nearest neighbors and next nearest neighbors are pairwise additive.

Implementation

The configurational integrals that define the free energies in Eqs. 8, 9, 11 and 12 are evaluated with a Monte Carlo integration scheme (Snurr et al., 1994; Clark et al., 1998). The simulation volume is discretized into cubelets, and for each Monte Carlo iteration, a cubelet is selected from a probability distribution function that has been assigned to each cubelet on the basis of the energy felt by a single molecule at the center of the cubelet. A molecule is then placed at random within the volume of the selected cubelet and the integrand is accumulated in a sum to yield the Monte Carlo estimate of the integral. The integration of the zeolite/sorbate configurational integrals converged after approximately 4 million iterations and were run for 10 million iterations, while the 2-body and 3-body integrations converged after at most 15 million iterations, but were run for up to 100 million iterations to provide good statistics. The cubelets of the simulation volume are assigned to regions corresponding to straight channels, zigzag channels, and channel intersections, as described elsewhere (Clark et al., 1998). The probe molecule used here to determine the volume of the different sites is SF_6. To maintain consistency, the same definitions of the sites are used for SF_6, neopentane, and mixtures of the two. It is interesting to note how the relative volumes of the sites depend on the probe molecule that is used. Clark et al. (1998) used argon as a probe when defining the sites in their work in silicalite. They report relative pore volumes of 13.0%, 38.2%, and 48.8% for the intersections, straight channels, and zigzag channels, respectively. We calculate relative pore volumes of 53.84%, 21.4%, and 24.8% based on SF_6. For a molecule in a zigzag channel, the interaction at one end of the zigzag channel (say, the "zig" end) with its surrounding sites is different than at the other end of the zigzag channel (the "zag" end). The free energies for both kinds of sites were evaluated, and the free energies containing a zigzag site are the arithmetic average of the two values.

We now discuss how the adsorption isotherm is calculated from the lattice model. For a single-component system, Snurr et al. (1994) used lattice grand canonical Monte Carlo simulations. The process by which this method should be extended to include multiple components is not obvious. Two possible algorithms are shown in Figure 4 for a binary mixture of components A and B. The first step in Algorithm 1 is to randomly choose a site. If it is occupied with a molecule of component A or B, then an attempt to delete it is made. The change in free energy, ΔA, associated with removing the molecule is calculated and the move is accepted with probability P_{del}. If the site is unoccupied, then with equal probability an attempt to insert a molecule of species A and B is made and accepted with probability P_{ins}. This procedure is similar to what physically occurs on a lattice site; a molecule must first vacate a site before another can replace it. The second algorithm introduces a swapping move to the procedure, where a molecule of component A is changed to a molecule of component B or vice versa. The first step in Al-

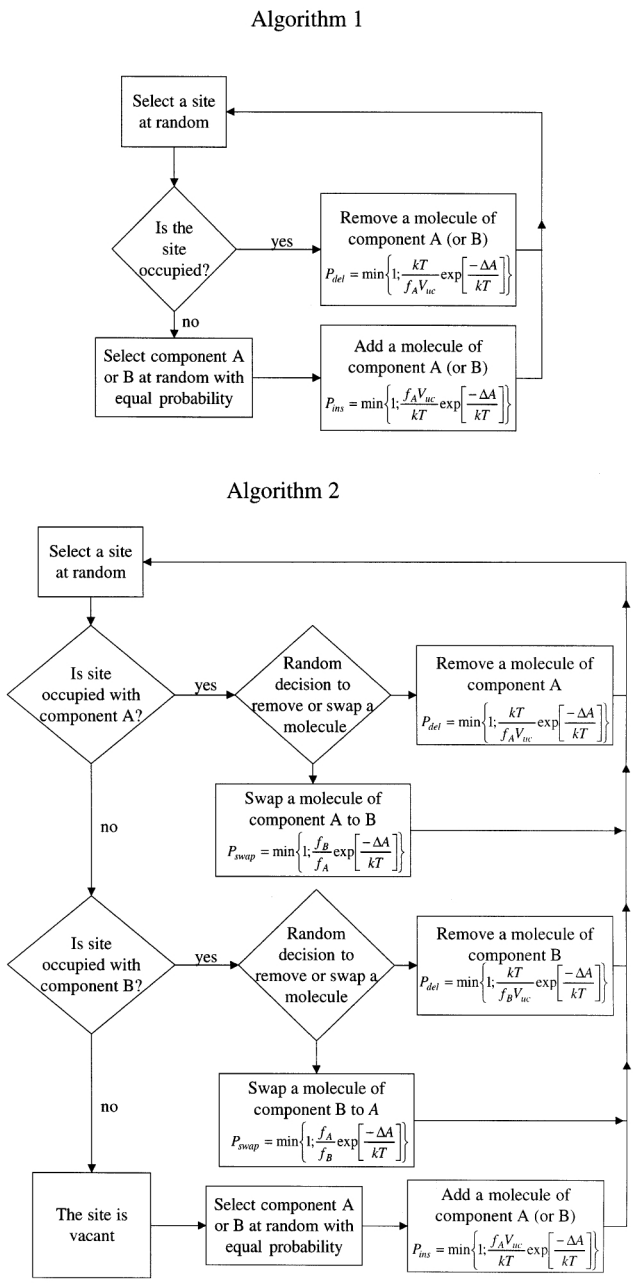

Figure 4. Two lattice GCMC algorithms for a binary mixture of components A and B.

Algorithm 2 satisfies microscopic reversibility and thus is the correct procedure.

gorithm 2 is to choose a site at random. If it is occupied with a molecule of A, then a random decision to remove the molecule or to swap it to a molecule of component B is made with equal probability. If the deletion of a molecule is to occur, then the change in energy of removing the molecule is calculated and the move is accepted with probability P_{del}. If the decision to swap is made, then the change in free energy of replacing a molecule of A for a molecule of B is calculated and the move accepted with probability P_{swap}. This procedure of possibly removing or swapping is similar if the site is occupied with a molecule of component B. If the site is unoccupied, then component A or B is selected with equal probability and an insertion is attempted; the change in free energy is calculated and the move accepted with probability P_{ins}. While the first algorithm may intuitively seem correct, only the second one satisfies microscopic reversibility and is thus the correct method of performing the moves (Czaplewski, 1998). The lattice model is actually a three state per site model where each adsorption site of the system makes transitions between the three states, A, B, or 0 (vacant). Typically, the lattice calculations converged after 100,000 to 1 million iterations and were run for 10 million iterations to provide good statistics. This typically required 100 to 500 s of CPU time on a desktop workstation, once the free energies were calculated.

Single-Component Results

The adsorption isotherms, along with other thermodynamic properties, calculated using lattice grand canonical Monte Carlo simulations are presented in this section for the adsorption of the single components SF_6 and neopentane in silicalite. Mixture results are presented in the following section. We also performed atomistic GCMC simulations on the same systems, and the results serve as a test of the lattice model. Therefore, the goal of this section is to show how well the lattice model is able to reproduce the results of the atomistic GCMC method but in a fraction of the computational run-time.

Although the effective diameter of neopentane is approximately 6.2 Å and the pore dimensions of the straight and zigzag channels are 5.4×5.6 Å and 5.1×5.4 Å, respectively, experimental data confirm that neopentane does adsorb into silicalite (Flanigen et al., 1978; Otto et al., 1991). A very limited amount of experimental adsorption data exists for neopentane in silicalite and therefore no comparison with simulation results was possible. Experimental results for the adsorption of SF_6 also exist, and a comparison shows that both the lattice and the atomistic GCMC models overpredict the Henry's constant and underpredict the saturation loading with the parameters used here (Dunne et al., 1996; Sun et al., 1998; Siperstein et al., personal communication, 1998). However, as stated, the primary goal of this study is to determine the ability of the hierarchical approach to reproduce atomistic simulation results for single-component and binary adsorption. The atomistic simulations provide an exact solution for the molecular model, while the lattice approach introduces certain approximations in order to achieve a solution with less computational effort. By comparing the two approaches, we can assess the effect of the simplifying assumptions invoked in the lattice model.

The free energies for the adsorption of SF_6 in silicalite calculated from Eqs. 8, 9, 11 and 12 using the atomistic representation are shown in Table 2. The relatively large, negative values of the zeolite/sorbate energies, the 1-body free energy, predict the favorable adsorption of SF_6 with a fairly even distribution throughout the three adsorption locations. At low loadings, the intersections are more favorable and thus should fill more rapidly than the S and Z sites, but this is only a slight preference. Both the entropic and enthalpic effects of adsorption from the gas phase are included by definition in the values of the free energies. The changes in potential en-

Table 2. One-, Two-, and Three-Body Free Energies in kJ/mol for the Adsorption of SF_6 in Silicalite at 293, 328, 343, and 373 K

Temp.	A_I	A_S	A_Z
293 K	−18.44	−16.27	−17.05
328 K	−16.59	−13.93	−14.71
343 K	−15.82	−12.94	−13.72
373 K	−14.27	−10.98	−11.76

Temp.	A_{IS}	A_{IZ}	A_{I_I}	A_{S_S}	A_{Z_Z}	A_{S_Z}
293 K	0.06	−1.02	−0.11	−0.19	−0.16	−0.53
328 K	0.21	−0.90	−0.11	−0.19	−0.17	−0.54
343 K	0.28	−0.85	−0.11	−0.19	−0.17	−0.54
373 K	0.37	−0.75	−0.11	−0.27	−0.18	−0.54

Temp.	A_{ISI}	A_{SIS}	A_{IZI}	A_{ZIZ}	A_{SIZ}
293 K	1.27	0.35	−0.47	0.07	0.19
328 K	1.32	0.36	−0.56	0.04	0.18
343 K	1.34	0.37	−0.57	0.05	0.20
373 K	1.38	0.55	−0.59	0.08	0.22

ergy and entropy a molecule undergoes when it is adsorbed from the gas phase are determined by plotting the ΔA's from Table 2 vs. the temperature and using the equation $\Delta A = \Delta U - T\Delta S$. They are reported in Table 3. Based on the relative volumes of the adsorption sites as defined earlier, it is intuitively expected that the intersections are the most entropically favorable and that the S and Z sites have similar values for ΔS. The values of ΔU are in good agreement with the average zeolite/sorbate potential energy, $\langle \mathfrak{V}^{zs} \rangle$, calculated in both the atomistic GCMC simulations and in the free-energy calculations.

As loadings increase, the effects of the sorbate/sorbate interactions increase in significance. These two-body free energies are one to two orders of magnitude smaller than the 1-body energies and all but the IS interaction are attractive (Table 2). The IS free energy is the first sign of a repulsion generated between two occupied sites. The average sorbate/sorbate potential energy, $\langle \mathfrak{V}^{ss} \rangle$, has been calculated between all of the pairs of molecules along with the average distance, $\langle d \rangle$, that separates the two molecules. These quantities are obtained during the calculation of the free energies. At 293 K, the average separation distance for the IS pair of molecules, 5.90 Å, is smaller than that for the IZ pair (Table 4), and the average sorbate/sorbate potential energy of the IS pair is less attractive, −1.28 kJ/mol, than that for the IZ pair, −1.39 kJ/mol. When examining the two-body free energies of next nearest-neighbor sites, I__I, S__S, Z__Z, and S__Z, it is important to remember that the first three pairs are positioned linearly within the zeolite pore system, while the S and the Z sites are at right angles to each other. The S and Z sites are closer to each other than the others, and the value of their two-body free energy is more attractive than the others. The free energies of three adjacent occupied sites, the 3-body free energies, are all repulsive except for the IZI triplet, and are essentially the same order of magnitude as the two-body free energies. Again, the most repulsive triplets, ISI and SIS, are those that include the IS pair. The average distance between the I and S molecules calculated for the ISI and SIS triplets are 5.63 Å and 5.78 Å, respectively. It is interesting to note the decrease in the average separation distance and the increase in the repulsion of the free energy as compared to those of only two adjacent molecules. These distances between the molecules in I and S sites are 0.2 Å to 0.6 Å less than the average distances of the molecules in I and Z sites of the other triplets, whose free energies are more attractive. This is exactly the type of 3-body repulsion hypothesized by Snurr et al. (1994).

Table 3. Enthalpies and Entropies of Adsorption in Silicalite for SF_6*

	Intersection	Straight	Zigzag
ΔU	−33.74	−35.64	−36.42
ΔS	−52.23	−66.15	−66.15

*The enthalpies are reported in kJ/mol, and the entropies are reported in J/mol/K.

Table 4. Average Distance in Angstroms Between All of the Pairs and Triplets of SF_6 Molecules at 293 K

Pairs of Sites	I_I	IS	IZ	S_S	S_Z	Z_Z
$\langle d_{12} \rangle$	10.73	5.91	6.17	9.91	8.02	10.38

Triplets of Sites	ISI	SIS	IZI	ZIZ	SIZ
$\langle d_{12} \rangle$	5.63	5.78	6.17	6.09	5.89
$\langle d_{23} \rangle$	5.63	5.80	5.97	6.21	6.14
$\langle d_{13} \rangle$	11.15	11.21	11.54	10.78	8.43

The Henry's constant and the isosteric heat at infinite dilution of SF_6 in silicalite were calculated from the free energies in Table 2 using analytical expressions given by Snurr et al. (1994). At 293 K, the Henry's constant has a value of 5.22×10^4 mg/(g·atm). The Henry's constants generated using the lattice model agree exactly with those calculated from the atomistic GCMC model. The isosteric heat of 37.55 kJ/mol at 293 K is also in agreement with the atomistic GCMC simulation. At infinite dilution, the approximations that were made in the lattice model do not yet play a role, and therefore exact agreement is expected.

The zeolite/sorbate free energies and the free energies between pairs and triplets of molecules were used as inputs for lattice grand canonical Monte Carlo simulations, and the single-component adsorption isotherms were calculated. Figure 5 shows the isotherms for SF_6 at 293 K and 373 K in silicalite (3-body Lattice). In order to study the impact the different free energies had on the isotherm, the isotherms were also calculated using only the 1-body and the nearest-neighbor two-body free energies (2-body Lattice) and calculated using only the 1-body free energies (1-body Lattice). An atomistic GCMC simulation of an identical system was performed and serves as a basis of comparison for all three of the lattice model simulations. At loadings of less than one molecule per unit cell, all of the models are in very good agreement. Then as the loading increases, the molecules begin to feel the effects of the neighboring molecules. The 1-body lattice model is the first to deviate from the other models, since it only accounts for the interactions the sorbed molecule has with the zeolite structure. The 2-body lattice model does a better job of calculating the average loading, but also underestimates the value calculated by the atomistic model. However,

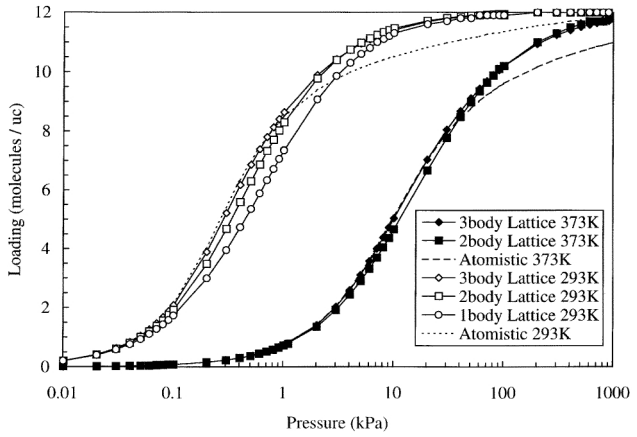

Figure 5. Adsorption isotherms for SF_6 in silicalite at 293 and 373 K.

The 3-body Lattice results were generated by the hierarchical model using all of the one-, two-, and three-body free energies. The 2-body Lattice results were generated by the hierarchical lattice model using only the 1-body and the adjacent neighbor two-body free energies. The 1-body Lattice results were generated using only the zeolite/sorbate free energies. The atomistic results were generated using atomistic GCMC.

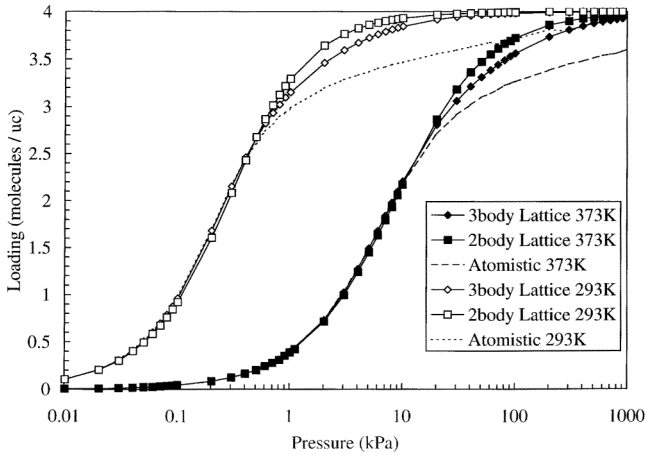

Figure 6. Adsorption isotherm at 293 and 373 K for SF_6 in the intersections of silicalite.

Good agreement between the lattice model and the atomistic GCMC results is obtained at lower loadings, while the models deviate at higher loadings.

the three-body lattice model calculates an average loading that is in reasonably good agreement with the atomistic GCMC model until approximately eight molecules per unit cell. At this loading, the 3-body model begins to overpredict the atomistic model average loading, as do the 2-body and 1-body lattice models. The atomistic model ultimately predicts saturation of the system at 12 molecules per unit cell, in agreement with the lattice models. However, the atomistic model predicts saturation at a much higher pressure than the lattice models.

The loadings of the individual sites, I, Z, and S, are shown in Figures 6–8, respectively. As predicted by the values of the free energies, the intersections begin to fill first, slightly ahead of the zigzag channels and then the straight channels. Overall, the 3-body lattice is an improvement from the two-body lattice models. The loading in the zigzag channel calculated by the three-body lattice model agrees well with the atomistic GCMC model throughout the entire pressure range. The loadings of the intersection sites agree well until a loading of about 2.5 molecules per unit cell. Here, and in the straight channels, the lattice model calculates an average loading that is too large compared to the atomistic GCMC values at loadings above 2.5 molecules per unit cell. It is not clear why the disagreement only occurs in the straight channels and the intersections and not the zigzag channels.

At saturation, an intersection has four occupied adjacent neighbor sites. Therefore, it is possible that 4-body free energies or higher-order effects become significant at higher loadings and would be repulsive enough to force the system to a lower average loading in agreement with the atomistic GCMC results. Another source of the deviations was also examined. The atomistic GCMC results indicate that only one molecule adsorbs in a given site, since there are four of each site per unit cell and the site loadings plateau at four molecules per unit cell. To test this further, the free energy of two molecules occupying a single site was calculated for each site and found to be greater than +19 kJ/mol, indicating that it would be extremely unfavorable to place two molecules in one site. Since there was a significant improvement of the 3-body lattice model over the 2-body lattice model, it seems reasonable to conclude that four- or five-body effects would improve the model at loadings approaching saturation.

The second system studied was neopentane in silicalite. The atomistic model was used to calculate the free energies for the adsorption of neopentane in silicalite, shown in Table 5. The free energies indicate favorable adsorption of neopentane in the intersections, but adsorption in the straight and zigzag channels is extremely unfavorable, signified by the large positive values of the free energies. As expected, the free en-

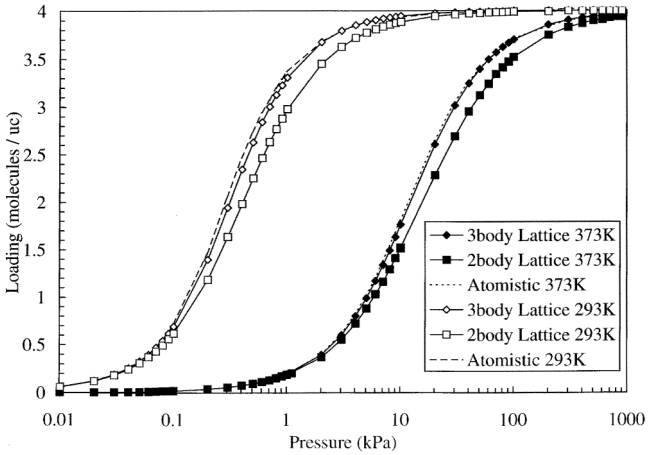

Figure 7. Adsorption isotherm at 293 and 373 K for SF_6 in the zigzag channels of silicalite.

Good agreement between the lattice and atomistic results is achieved for the zigzag channels over the entire pressure range.

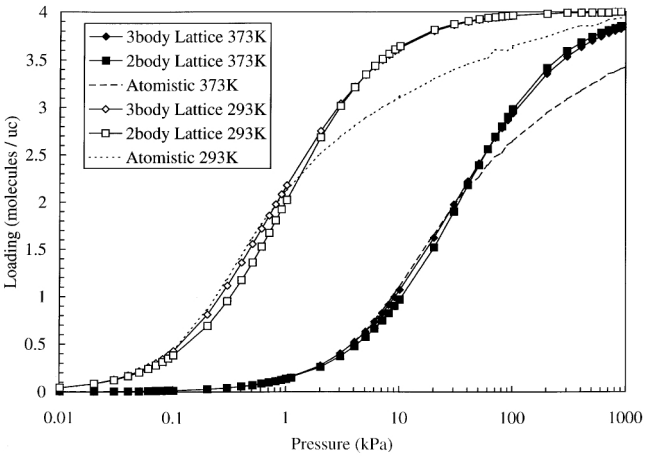

Figure 8. Adsorption isotherm at 293 and 373 K for SF_6 in the straight channels of silicalite.

Similar to the intersections, the results of the two models agree at lower loadings and deviate at higher loadings.

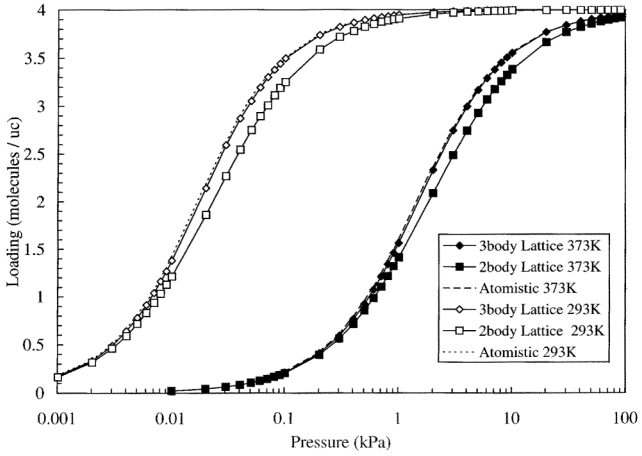

Figure 9. Adsorption isotherms for neopentane in silicalite at 293 and 373 K.

The 3body and the atomistic GCMC results agree very well with each other. The improvement of the lattice model with the addition of the three-body free energies is well demonstrated, compared to the 2-body Lattice results.

ergy between two occupied adjacent sites is also very repulsive, along with all of the free energies of the triplets. The only attractive free energies are between pairs of next nearest-neighbor sites, and their values are up to two orders of magnitude smaller than the one-body free energies. The lattice model gives a Henry's constant for neopentane in silicalite at 373 K of 2.74×10^5 mg/(g·atm), again in excellent agreement with the atomistic GCMC simulation. The isosteric heat was determined to be 49.87 kJ/mol, also agreeing exactly with the atomistic results. Figure 9 shows the adsorption isotherms of neopentane at 293 K and 373 K. The isotherms reach a saturation loading of four molecules per unit cell, and from the site loading data (not shown) it was determined that all of the molecules are located in the intersections, as predicted by the values of the free energies. The 3-body lattice model for this system gives very good agreement with the atomistic GCMC results and improves over the results obtained by excluding the three-body free energies and the next nearest-neighbor free energies. By extending the lattice model to include the 3-body free energies and the next nearest-neighbor free energies, the lattice model gives good agreement with the GCMC results.

Table 5. One-, Two-, and Three-Body Free Energies in kJ/mol for the Adsorption of Neopentane in Silicalite

Temp.	A_I	A_S	A_Z
293 K	−25.31	65.76	58.94
328 K	−22.66	68.79	62.26
343 K	−21.58	70.08	63.67
373 K	−19.38	72.64	66.45

Temp.	A_{IS}	A_{IZ}	A_{I_I}	A_{S_S}	A_{S_Z}	A_{Z_Z}
293 K	8.34	6.90	−0.32	−0.52	−1.25	−0.31
328 K	8.70	6.95	−0.38	−0.55	−1.26	−0.31
343 K	8.87	6.97	−0.32	−0.53	−1.26	−0.31
373 K	9.17	7.01	−0.32	−0.53	−1.26	−0.31

Temp.	A_{ISI}	A_{SIS}	A_{IZI}	A_{ZIZ}	A_{SIZ}
293 K	42.20	4.71	2.66	0.60	0.34
328 K	42.19	4.81	2.81	0.61	0.37
343 K	42.18	4.78	2.73	0.61	0.37
373 K	42.14	4.82	2.78	0.61	0.38

Binary Mixture Results

Systems containing both neopentane and SF_6 were also examined using the lattice model. Multicomponent systems require the calculation of many more free energies than single-component systems, because of the increased number of sorbate interaction combinations. The zeolite/sorbate free energies and the free energies of the pairs and triplets of similar molecules were taken from the single-component calculations. What remained to be calculated were the two-body and three-body free energies for the combinations of dissimilar components. This amounted to 13 additional two-body free energies and 32 additional three-body free energies to be calculated to completely describe the system. The calculations of the free energies are the computationally intensive portion of the hierarchical approach. Thus an attempt was made to reduce the number of free-energy calculations. Since the neopentane molecules only adsorb in the intersections in the pure-component system (due to the large, repulsive S and Z free energies), only free energies that contain neopentane molecules in the intersections ever make significant contributions to the equilibrium calculations for the mixture. This assumption reduced the required number of two-body and three-body free energies calculations for the mixture to those shown in Table 6. The nearest-neighbor two-body free energies for the dissimilar species are both repulsive. The next nearest-neighbor two-body free energy, I__I, for the dissimilar species in intersections is slightly attractive, similar to the single-component neopentane system. All but the SF_6–SF_6–neopentane IZI three-body energies are repulsive, and as expected from the difference in size, having two neopentane molecules in a triplet is more repulsive than sim-

Table 6. Two- and Three-Body Free Energies in kJ/mol for the Adsorption of the Mixture of SF_6 and Neopentane in Silicalite

Neopentane–SF_6			
Temp.	A_{I_I}	A_{IS}	A_{IZ}
293 K	−0.20	1.79	0.12
328 K	−0.20	2.03	0.24
343 K	−0.20	2.13	0.30
373 K	−0.20	2.29	0.41

Neopentane–SF_6–Neopentane		
Temp.	A_{ISI}	A_{IZI}
293 K	17.54	1.46
328 K	17.63	1.67
343 K	17.68	1.61
373 K	17.76	1.69

SF_6–Neopentane–SF_6			
Temp.	A_{SIS}	A_{ZIZ}	A_{SIZ}
293 K	0.42	0.14	0.29
328 K	0.44	0.15	0.30
343 K	0.45	0.16	0.30
373 K	0.63	0.17	0.31

SF_6–SF_6–Neopentane		
Temp.	A_{ISI}	A_{IZI}
293 K	3.81	−0.05
328 K	3.96	−0.05
343 K	4.02	−0.04
373 K	4.13	−0.02

ply having one. These free energies were entered into the lattice model and isotherms were generated at three different values of the total pressure.

The adsorption of neopentane and SF_6 at 293 K and at a constant total pressure of 0.1 kPA was simulated using the lattice model and the full atomistic GCMC algorithm. The mole fraction of neopentane in the gas phase, y_N, was varied between zero and one, and the total loading of each component is shown in Figure 10. The results from the lattice model match those of the atomistic GCMC simulation well. There is good agreement for the neopentane loading, and the SF_6 data also exhibit reasonably good agreement between the two methods. The loading of the individual sites is shown in Figure 11. The results of the lattice model match those of the atomistic GCMC very well. As in the single-component system, there is no adsorption of neopentane molecules in the channel sites (not shown); all of the neopentane adsorbs in the intersection sites. The adsorption of the SF_6 into the three different sites followed the same trend as the single-component results, the intersections having the highest loading, then the zigzag and straight channels. The favorable adsorption of neopentane at this total pressure is evident in the *xy*-diagram of the system shown in Figure 12. This is a plot of the mole fraction of neopentane in the adsorbed phase, x_N, vs. the gas-phase mole fraction of neopentane. With the equilibrium curve lying to the left of the $x = y$ line, it is shown that the adsorption of neopentane is more favorable than SF_6 at 0.1 kPa.

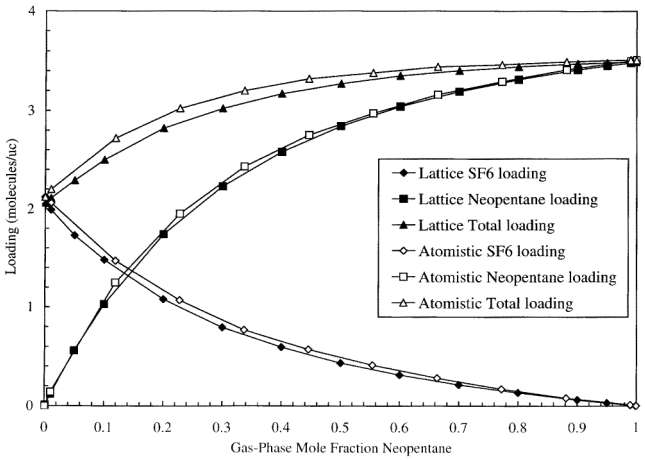

Figure 10. Adsorption of SF_6 and neopentane in silicalite at 0.1 kPa and 293 K as a function of gas-phase composition.

Relatively good agreement is achieved between the lattice model and the atomistic GCMC simulations.

Simulations were also performed at a constant total gas-phase pressure of 1.0 kPa using the lattice and the atomistic models. The loading of each component and the total for the system are shown in Figure 13. Again, very good agreement between the lattice model and the atomistic GCMC simulations were achieved for neopentane adsorption, and reasonably good agreement for SF_6 adsorption. The deviations occurred primarily in the zigzag channels, with some initial deviations occurring in the intersections and at intermediate y_N in the straight channels (Figure 14). As the mole fraction of neopentane increases, SF_6 in the intersections is displaced by neopentane. The SF_6 in the straight channels also appears

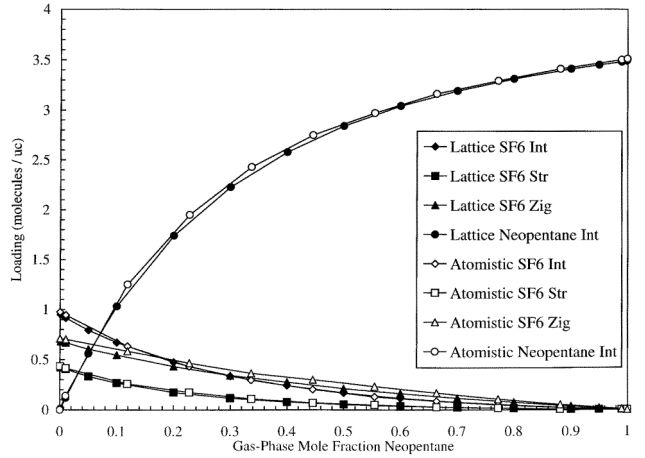

Figure 11. Adsorption of SF_6 and neopentane in the different adsorption sites at 0.1 kPa and 293 K as a function of gas-phase composition.

The loadings of the intersections and channels with SF_6 and the loading of the intersections with neopentane is shown. Neopentane does not adsorb in the channels of silicalite. Good agreement between the two adsorption models is achieved.

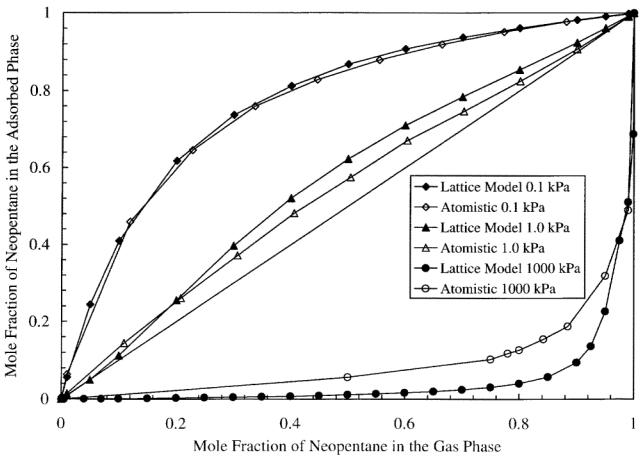

Figure 12. *xy*-Diagram of SF_6 and neopentane at 293 K and at 0.1, 1.0, and 1,000 kPa.

The data show that at low total pressure the adsorption of neopentane is favored, and as the total pressure increases, the favorability of SF_6 adsorption increases.

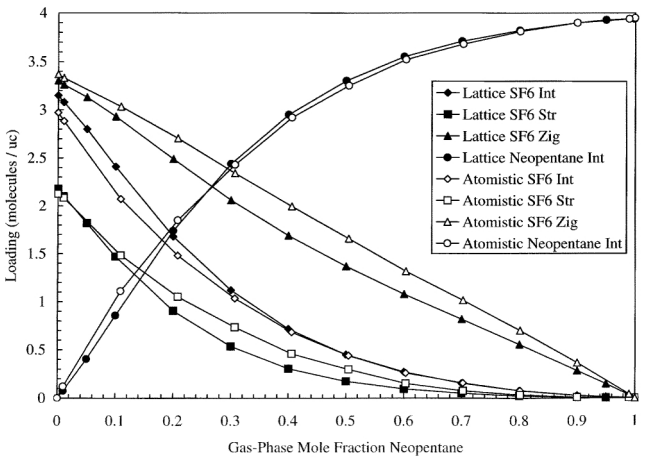

Figure 14. Adsorption of SF_6 and neopentane in the different adsorption sites at 1.0 kPa and 293 K as a function of gas-phase composition.

The displacement of SF_6 from the intersections by the neopentane molecules is shown. The loading of SF_6 in the straight channels also appears to be affected by the addition of neopentane. The SF_6 in the zigzag channels appears less affected.

to be affected by the presence of neopentane, while the effect is less apparent in the zigzag channels. Neopentane is still slightly more favorably adsorbed than SF_6, but the equilibrium adsorption curve lies closer to the $x = y$ line in Figure 12, signaling an increasing favorability of SF_6 adsorption with increased pressure.

Simulations of SF_6 and neopentane in silicalite were also performed at a constant total gas-phase pressure of 1000 kPa using both models. Again, the total loadings of each component and the total loading of the system were calculated (Figure 15). At this higher total pressure, only qualitative agreement between the two models is achieved. The lattice model overpredicts the loading of SF_6 by up to 2 molecules per unit cell and by up to 1 molecule per unit cell for the neopentane. The overprediction of the loading occurs primarily in the intersections and straight channels, as shown in Figure 16. As the neopentane molecules displace the SF_6 molecules in the intersections, deviations between the models exist in both the intersections and the straight channels. The presence of neopentane in the intersections appears to displace some of the SF_6 molecules in the straight channels, and the models do not agree upon the magnitude of this displacement. Very good agreement is achieved between the models for the SF_6 loading in the zigzag channels, which seems relatively unaffected by the presence of the neopentane in the intersections. At this highest total pressure, the adsorption of SF_6 is strongly favored over the adsorption of the neopentane. As the mole fraction of the neopentane in the gas phase increases, the mole fraction of neopentane in the adsorbed

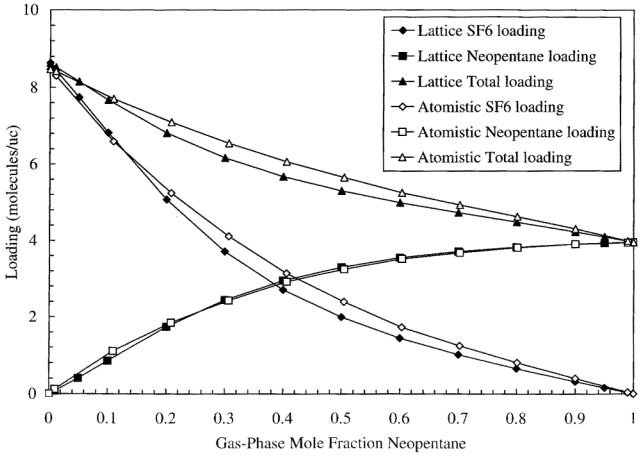

Figure 13. Adsorption of SF_6 and neopentane in silicalite at 1.0 kPa and 293 K as a function of gas-phase composition.

Good overall agreement between models is achieved, with some deviations occurring in the SF_6 loading.

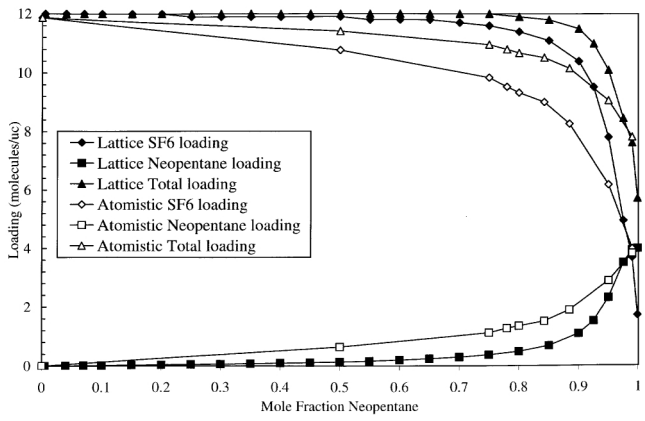

Figure 15. Adsorption of SF_6 and neopentane in silicalite at 1,000 kPa and 293 K as a function of gas-phase composition.

Only qualitative agreement between the two models is achieved at this relatively high total pressure.

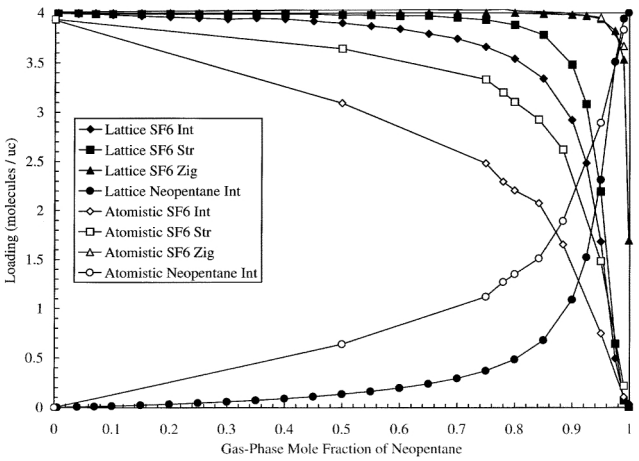

Figure 16. Adsorption of SF_6 and neopentane in the different adsorption sites at 1,000 kPa and 293 K as a function of gas-phase composition.

Only qualitative agreement between the models is observed in all of the adsorption sites except for SF_6 in the zigzag channels, where very good agreement is achieved.

phase increases much more slowly, and thus the data of the *xy*-diagram (Figure 12) lie to the right of the $x = y$ equilibrium line.

The lattice model produces results that are in good overall agreement with the atomistic GCMC calculations, and it has the advantage of being less computationally intensive. The free-energy calculations constitute the major computational expense in the hierarchical approach. Once tabulated, an isotherm over the entire pressure range can be generated in less than 3 h of CPU time on a desktop workstation. For atomistic GCMC simulations, the computational time increases tremendously as loading is increased due to the increase in the number of iterations required for convergence and the increase in the number of sorbate/sorbate calculations between the greater number of molecules. The lattice model is about an order of magnitude more efficient computationally than the atomistic GCMC simulations. For example, the GCMC simulations of the three mixtures took a total CPU time of 161 h on a 500-MHz workstation. If the CPU time required for the single-component free energies is excluded, the lattice model takes about 11 h of CPU time, or 39 h if all of the single-component calculations are included.

Conclusion

The hierarchical lattice approach first developed by Snurr et al. (1994) for the adsorption of benzene in silicalite has been extended to multicomponent systems. The grand partition function for a multicomponent system has been derived in terms of the free energies for adsorption in the different sites of silicalite and for sorbate/sorbate interactions. Free energies for next nearest-neighbor interactions and for triplets of molecules occupying three adjacent sites have also been included. The role of these higher-order free energies in determining equilibrium properties has been investigated. The free energies are calculated from short simulations using a detailed atomistic model and are then used within a simpler lattice model to obtain the adsorption isotherm and other properties of interest.

The addition of the three-body and nonadjacent two-body free energies makes a significant improvement in the results from the lattice model when compared to fully atomistic GCMC simulations for SF_6 and neopentane in silicalite. In both of the single-component systems, the three-body lattice model agrees well with the atomistic GCMC results, improving upon the 2-body lattice results. In the SF_6 system, it is proposed that four-body or five-body free energies may be required to better describe the system at the highest loadings. Good agreement is achieved between the lattice model and the atomistic GCMC model in predicting the adsorption of mixtures at constant total pressures of 0.1 kPa, 1.0 kPa, and of 1,000 kPa at 293 K. At the lowest total pressure, neopentane adsorbs more strongly, but as pressure increases, the favorability of SF_6 adsorption increases. The hierarchical approach proves to be a valuable adsorption simulation technique, yielding the same results as atomistic GCMC simulations but in a fraction of the computer time.

Acknowledgment

This work was supported by a CAREER grant from the National Science Foundation, Division of Chemical and Transport Systems.

Literature Cited

Breck, D., *Zeolite Molecular Sieves*, Wiley-Interscience, New York (1974).

Chiang, A. S. T., C. Lee, W. Rudzinski, J. Narkiewicz-Michalek, and P. Szabelski, "Energy and Structure Heterogeneities for the Adsorption in Zeolites," *Stud. Surf. Sci. Cat.*, **104**, 519 (1997).

Clark, L. A., A. Gupta, and R. Q. Snurr, "Siting and Segregation Effects of Simple Molecules in Zeolites MFI, MOR and BOG," *J. Phys. Chem. B*, **102**, 6720 (1998).

Czaplewski, K. F., "Simulation of Binary Adsorption Thermodynamics in Silicalite Using a Hierarchical Approach," MS Thesis, Northwestern University, Evanston, IL (1998).

Davis, M. E., "Zeolites and Molecular Sieves: Not Just Ordinary Catalysts," *Ind. Eng. Chem. Res.*, **30**, 1675 (1991).

Dunne, J. A., R. Mariwala, M. Rao, S. Sircar, R. J. Gorte, and A. L. Myers, "Calorimetric Heats of Adsorption and Adsorption Isotherms: 1. O_2, CO_2, CH_4, C_2H_6, and SF_6 on Silicalite," *Langmuir*, **12**, 5888 (1996).

Dunne, J. A., and A. Myers, "Adsorption of Gas Mixtures in Micropores: Effect of Difference in Size of Adsorbate Molecules," *Chem. Eng. Sci.*, **49**, 2941 (1994).

Dunne, J. A., and A. L. Myers, "Simulation of Adsorption of Liquid Mixtures of N_2 and O_2 in a Model Faujasite Cavity at 77.5 K," *Adsorption*, **2**, 41 (1996).

Dunne, J. A., M. Rao, S. Sircar, R. J. Gorte, and A. L. Myers, "Calorimetric Heats of Adsorption and Adsorption Isotherms: 3. Mixtures of CH_4 and C_2H_6 in Silicalite and Mixtures of CO_2 and C_2H_6 in NaX," *Langmuir*, **13**, 4333 (1997).

Flanigen, E. M., J. M. Bennett, R. W. Grose, J. P. Cohen, R. L. Patton, R. M. Kirchner, and J. V. Smith, "Silicalite, a New Hydrophobic Crystalline Silica Molecular Sieve," *Nature*, **271**, 512 (1978).

Heuchel, M., R. Q. Snurr, and E. Buss, "Adsorption of CH_4-CF_4 Mixtures in Silicalite: Simulation, Experiment and Theory," *Langmuir*, **13**, 6795 (1997).

Hill, T. L., *Statistical Mechanics*, McGraw-Hill, New York (1956).

Hill, T. L., *An Introduction to Statistical Thermodynamics*, Addison-Wesley, Reading, MA (1962) (reprint published by Dover Publications, Mineola, New York, 1986).

Jameson, C. J., A. K. Jameson, and H. M. Lim, "Competitive Adsorption of Xenon and Argon in Zeolite NaA: 129Xe Nuclear Magnetic Resonance Studies and Grand Canonical Monte Carlo Simulations," *J. Chem. Phys.*, **104**, 1709 (1996).

Jameson, C. J., A. K. Jameson, and H. M. Lim, "Competitive Adsorption of Xenon and Krypton in Zeolite NaA: 129Xe Nuclear Magnetic Resonance Studies and Grand Canonical Monte Carlo Simulations," *J. Chem. Phys.*, **107**, 4364 (1997).

June, R. L., A. T. Bell, and D. N. Theodorou, "Transition-State Studies of Xenon and SF_6 Diffusion in Silicalite," *J. Phys. Chem.*, **95**, 8866 (1991).

Karavias, F., and A. L. Myers, "Monte Carlo Simulation of Binary Gas Adsorption in Zeolite Cavities," *Mol. Simul.*, **8**, 51 (1991).

Kiselev, A. V., A. A. Lopatkin, and A. A. Shulga, "Molecular Statistical Calculation of Gas Adsorption by Silicalite," *Zeolites*, **5**, 261 (1985).

Lachet, V., A. Boutin, B. Tavitian, and A. Fuchs, "Grand Canonical Monte Carlo Simulations of Adsorption of Mixtures of Xylene Molecules in Faujasite Zeolites," *Faraday Discuss.*, **106**, 307 (1997).

Lee, C.-K., A. S. T. Chiang, and F. Wu, "Lattice Model for the Adsorption of Benzene in Silicalite I," *AIChE J.*, **38**, 128 (1992).

Macedonia, M. D., and E. J. Maginn, "Pure and Binary Component Sorption Equilibria of Light Hydrocarbons in the Zeolite Silicalite from Grand Canonical Monte Carlo Simulations," *Fluid Phase Equil.*, **158–160**, 19 (1999).

Maddox, M., and J. Rowlinson, "Computer Simulation of the Adsorption of a Fluid Mixture in Zeolite Y," *J. Chem. Soc. Faraday Trans.*, **89**, 3619 (1993).

Olson, D. H., G. T. Kokotailo, S. L. Lawton, and W. M. Meier, "Crystal Structure and Structure-Related Properties of ZSM-5," *J. Phys. Chem.*, **85**, 2238 (1981).

Otto, K., C. N. Montreuil, O. Todor, R. W. McCabe, and H. S. Gandhi, "Adsorption of Hydrocarbons and Other Exhaust Components on Silicalite," *Ind. Eng. Chem. Res.*, **30**, 2333 (1991).

Razmus, D., and C. Hall, "Prediction of Gas Adsorption in 5A Zeolite Using Monte Carlo Simulation," *AIChE J.*, **37**, 769 (1991).

Reid, R. C., J. M. Prausnitz, and B. E. Poling, *The Properties of Gases and Liquids*, 4th ed., McGraw-Hill, New York (1987).

Rudzinski, W., J. Narkiewicz-Michalek, P. Szabelski, and A. S. T. Chiang, "Adsorption of Aromatics in Zeolites ZSM-5: A Thermodynamic-Calorimetric Study Based on the Model of Adsorption on Heterogeneous Adsorption Sites," *Langmuir*, **13**, 1095 (1997).

Ruthven, D. M., *Principles of Adsorption and Adsorption Processes*, Chap. 5, Wiley-Interscience, New York (1984).

Snurr, R. Q., A. T. Bell, and D. N. Theodorou, "Prediction of Adsorption of Aromatic Hydrocarbons in Silicalite from Grand Canonical Monte Carlo Simulations with Biased Insertions," *J. Phys. Chem.*, **97**, 13742 (1993).

Snurr, R. Q., A. T. Bell, and D. N. Theodorou, "A Hierarchical Atomistic/Lattice Simulation Approach for the Prediction of Adsorption Thermodynamics of Benzene in Silicalite," *J. Phys. Chem.*, **98**, 5111 (1994).

Sun, M., D. Shah, H. Xu, and O. Talu, "Adsorption Equilibria of C_1 to C_4 Alkanes, CO_2, SF_6 on Silicalite," *J. Phys. Chem. B*, **102**, 1466 (1998).

Van Tassel, P. R., H. T. Davis, and A. V. McCormick, "New Lattice Model for Adsorption of Small Molecules in Zeolite Micropores," *AIChE J.*, **40**, 925 (1994a).

Van Tassel, P. R., H. T. Davis, and A. V. McCormick, "Adsorption Simulations of Small Molecules and Their Mixtures in a Zeolite Micropore," *Langmuir*, **10**, 1257 (1994b).

Manuscript received Dec. 28, 1998, and revision received June 28, 1999.